Draft version October 13, 2011
Preprint typeset using LaTeX style emulateapj v. 11/10/09



# A *SWIFT* LOOK AT SN 2011fe: THE EARLIEST ULTRAVIOLET OBSERVATIONS OF A TYPE Ia SUPERNOVA

Peter J. Brown[1] Kyle S. Dawson[1], Massimiliano de Pasquale[2], Caryl Gronwall[3,4], Stephen Holland[5,6,7], Stefan Immler[5,8,9], Paul Kuin[10], Paolo Mazzali[11,12], Peter Milne[13], Samantha Oates[9], & Michael Siegel[2]

*Draft version October 13, 2011*

## ABSTRACT

We present the earliest ultraviolet (UV) observations of the bright Type Ia supernova SN 2011fe/PTF11kly in the nearby galaxy M101 at a distance of only 6.4 Mpc. It was discovered shortly after explosion by the Palomar Transient Factory and first observed by Swift/UVOT about a day after explosion. The early UV light is well-defined, with ∼20 data points per filter in the 5 days after explosion. With these early UV observations, we extend the near-UV template of SNe Ia to earlier times for comparison with observations at low and high redshift and report fits from semi-empirical models of the explosion. We find the early UV count rates to be well fit by the superposition of two parabolic curves. Finally, we use the early UV flux measurements to examine a possible shock interaction with a non-degenerate companion. We find that even a solar mass companion at a distance of a few solar radii is unlikely at more than 95% confidence.

*Subject headings:* galaxies: distances and redshifts– supernovae: general–ultraviolet: general

## 1. EARLY OBSERVATIONS OF TYPE Ia SUPERNOVAE

Serendipitous discoveries of core-collapse supernovae (SNe) at very early times have been used to determine the early temperature of ejecta, the size of the SN ejecta, and the shock breakout, providing strong constraints on the progenitors. The shock breakout of SN 2008D (Soderberg et al. 2008) was observed in the X-ray, ultraviolet (UV), and optical bands by the *Swift* spacecraft (Gehrels et al. 2004) and the shock breakouts of several SNe IIP were found after the fact in UV observations from GALEX (Gezari et al. 2008). Rapid response observations of SN 2006aj by *Swift* were automatically triggered by the corresponding Gamma Ray Burst (GRB) 060218 (Campana et al. 2006). Promptly announced SN discoveries can also result in early *Swift* UV/X-ray observations (Roming et al. 2009; Gal-Yam et al. 2011).

For SNe Ia, early observations also offer clues into the nature of the progenitor system and properties of the SN explosion (e.g. Foley et al. 2011). While the shock breakout itself is expected to be extremely short (Piro, Chang, & Weinberg 2010), early observations do constrain the size and separation of a companion star (Kasen 2010; Brown et al. 2011, hereafter K10 and B11). In this letter we present results from very early *Swift* observations of SN 2011fe in the nearby galaxy M101, the earliest UV measurements to date for a SN Ia.

## 2. OBSERVATIONS

SN 2011fe, also known as PTF11kly, was discovered in M101 at a magnitude g=17.2, classified as a probable young Ia, and promptly announced by the Palomar Transient Factory (PTF; Law et al. 2009) on 2011 August 24 (Nugent et al. 2011). It was not detected by PTF to a limiting magnitude of 20.6 one day before, strongly constraining the explosion date. X-ray and UV observations were promptly requested from the *Swift* spacecraft, and observations began August 24.9. *Swift*'s Ultraviolet/Optical Telescope (UVOT; Roming et al. 2005) utilized the 6 broadband filters with the following central wavelengths ($\lambda_c$) and full-width half maximum (FWHM) in Angstroms: uvw2 ($\lambda_c$=1928; FWHM=657), uvm2 ($\lambda_c$=2246; FWHM=498), uvw1 ($\lambda_c$=2600; FWHM=693), u ($\lambda_c$=3465; FWHM=785), b ($\lambda_c$=4392; FWHM=975), and v ($\lambda_c$=5468; FWHM=769). Initial UVOT magnitudes were reported by Cenko et al. (2011b) as well as X-ray upper limits from *Swift*/XRT (Margutti & Soderberg 2011).

Following the announcement of the discovery of SN 2011fe, we requested daily *Swift* observations to monitor its UV and optical behavior. SN 2011fe rapidly brightened, necessitating several changes to the normal SN observing strategy and data reduction. After the first

[1] Department of Physics & Astronomy, University of Utah, 115 South 1400 East #201, Salt Lake City, UT 84112, USA
[2] Department of Physics and Astronomy, University of Nevada, Las Vegas - 4505 S. Maryland Parkway, Las Vegas, NV 89154, USA
[3] Department of Astronomy and Astrophysics, The Pennsylvania State University, 525 Davey Laboratory, University Park, PA 16802, USA
[4] Institute for Gravitation and the Cosmos, The Pennsylvania State University, University Park, PA 16802, USA
[5] Astrophysics Science Division, Code 660.1, 8800 Greenbelt Road Goddard Space Flight Centre, Greenbelt, MD 20771, USA
[6] Universities Space Research Association 10211 Wincopin Circle, Suite 500 Columbia, MD 21044, USA
[7] Centre for Research and Exploration in Space Science and Technology Code 668.8 8800 Greenbelt Road Goddard Space Flight Centre, Greenbelt, MD 20771, USA
[8] Department of Astronomy, University of Maryland, College Park, MD 20742, USA
[9] Center for Research and Exploration in Space Science and Technology, NASA Goddard Space Flight Center, Greenbelt, MD 20771, USA
[10] Mullard Space Science Laboratory, University College London, Holmbury St. Mary, Dorking Surrey, RH5 6NT, UK
[11] Max-Planck-Institut fr Astrophysik, Karl-Schwarzschild-Strasse 1, D-85748 Garching, Germany
[12] INAF-Osservatorio Astronomico, vicolo dellOsservatorio, 5, I-35122 Padova, Italy
[13] Steward Observatory, University of Arizona, Tucson, AZ 85719, USA

several observations we changed observing modes to use a smaller region of the CCD read out at a faster rate (3.6 ms compared to the normal 11.0 ms frame time) so the effects of coincidence loss could be corrected to a higher count rate (Poole et al. 2008). Observations with more than 0.95 counts per frame were discarded. The use of smaller hardware windows allowed us to follow it to magnitudes of 12.4, 12.4, and 10.8, in the u, b, and v filters, respectively. In the UV, count rates are much lower, but near peak the SN still required significant corrections to the UV rates and some frames were saturated in the uvw1 filter.

The adopted analysis uses a 5″circular aperture with which to measure the source counts, and otherwise follows the procedure of Brown et al. (2009). Pre-explosion images of M101 taken in 2007 March/April were used to subtract the underlying galaxy count rate. The coincidence loss corrected count rates are given in Table 1 along with the observed apparent magnitudes. The final data set uses over 500 individual exposures, including ∼20 points per filter in the first 5 days after explosion and ∼50 pre-maximum points per filter in the UV. The photometry is based on the UVOT photometric system of Poole et al. (2008) to be consistent with the existing sample of UVOT SN photometry (Brown et al. 2009; Milne et al. 2010, hereafter B09;M10). A Cepheid-based distance modulus of 29.04 ± 0.20 (6.4 Mpc; Shappee & Stanek 2011) is assumed for the absolute magnitudes. A small reddening of E(B-V)=0.01 is assumed for the Milky Way (Schlegel et al. 1998) and the host galaxy reddening is negligible (Li et al. 2011).

## 3. ANALYSIS

The excellent sampling of this data enables a detailed look at the early UV behavior for the extension of template light curves, an examination of the physical behavior, and constraints on single degenerate companions.

### 3.1. *Early UV light curves and colors*

Figure 1 displays the exquisitely sampled UVOT light curves of SN 2011fe. While the SN had already brightened to ∼15.7 mag in the optical ∼1 day after explosion, the first two exposures in uvm2 provided only 99% upper limits at mag 19.2 (corresponding to an absolute magnitude of -9.6 and a flux density of $\sim 5 \times 10^{-17}$ erg s$^{-1}$ cm$^{-2}$ Å$^{-1}$).

SNe Ia have long been characterized by their low UV flux relative to the optical at maximum light (Holm, Wu, & Caldwell 1974; Kirshner et al. 1993; Panagia 2003). The early observations of SN 2011fe reveal an even larger deficit of UV flux. This behavior extends the trends reported in M10 to earlier times. The right panel of Figure 1 shows the uvw1-v color evolution of SN 2011fe compared to the other SNe observed early by *Swift*/UVOT (B11).As with other SNe, the UV/optical flux ratio reaches a maximum a few days before optical maximum light. The early UV deficit is believed to be caused by a lack of heavy elements in the outermost layers ($> 12 - 15000$ km s$^{-1}$) of the SNe at early times. In this scenario, UV photons will be absorbed at smaller radii, and the outer layers do not have the composition to produce inverse flourescence (Mazzali 2000). As the SN photosphere recedes with time, UV photons will still be absorbed, but larger abundances of Fe, Co, Cr, Ti will be present near the photosphere. The optical lines of FeII, III, Co II, III, Ti II, CrII are expected to saturate, and fluorescence via UV lines should then become possible. As the SN approaches maximum optical light, a decrease in temperature leads again to a reddening in uvw1-v color.

SN 2011fe is significantly bluer than SN 2009ig at early times and follows the blue end of the SN sample. Combined with the detection of CII in the early spectra (Cenko et al. 2011b), this is consistent with the observation that SNe Ia with carbon usually have bluer NUV-optical color evolution (Thomas et al. 2011; Milne et al., 2012, in preparation).

It is essential to model the time evolution of SN Ia luminosity through template light curve to determine times of maximum light, interpolate light curves, differentiate between typical and atypical SNe, and define normal behavior for comparison with theoretical models. The first near-UV SN Ia template (F275W filter with peak wavelength = 2740 Å and FWHM=594 Å) was generated from International Ultraviolet Explorer (IUE) and Hubble Space Telescope (HST) observations of SNe 1990N and 1992A (Kirshner et al. 1993) . This served as an excellent template for early *Swift*/UVOT observations (Brown et al. 2005) without the stretching usually required in the optical to fit individual SNe. M10 improved upon this template using normal events observed by *Swift*/UVOT. Only the rapid declining SNe 2005ke (Immler et al. 2006) and 2007on (which were not included in the generation of the template) show significant deviations from it (M10).

The early observations of SN 2011fe give us the opportunity to extend that template to earlier times. To do so, we begin with the M10 templates for uvw1 and uvw2 and shift SN 2011fe in time and magnitude to give the minimum $\chi^2$ between the SNe and the template. A cubic polynomial is fit to the points to give the new pre-maximum template. The new uvw1 and uvw2 templates are given in Table 1 and displayed in the left panel of Figure 1. This extension is based only on one SN, but is consistent with other SNe Ia observed before maximum. The previous earliest UV observations from SN 2009ig (Foley et al. 2011;B11), can be stretched (i.e. scaling the time axis) to match this new template. The stretching must be done independently before and after maximum as in Hayden et al. (2010), as SN 2009ig rises more quickly but then fades more slowly.

Creating a template for the uvm2 filter is more difficult due to the variety seen in the peak times and light curve shapes (B09;M10). We leave a detailed study of the uvm2 light curves to future work, but the well sampled uvm2 light curves of SN 2011fe presented here should make an excellent comparison for other SNe.

### 3.2. *The Expanding Fireball Model and the Early UV Flux*

The early optical flux curves of SNe Ia are often assumed to follow the "expanding fireball" model described in Riess et al. (1999). Assuming that the flux arises from a quasi-blackbody observed on the Rayleigh-Jeans tail, the expanding photosphere would have an emitting area proportional to the square of the velocity and the square

of the time since explosion squared. If the temperature and velocity are relatively constant compared to the rapidly changing time since explosion, then those other terms can be assumed into a constant of proportionality. Specifically, the flux relates to the time since explosion approximately as $f = \alpha(t - t_0)^2$ (Riess et al. 1999; Garg et al. 2007; Ganeshalingam et al. 2011), where t is the observation date, $t_0$ is usually taken to be the date of explosion, and $\alpha$ is a constant that absorbs the distance, temperature, velocity, and other factors. The flux is zero for $t < t_0$. The assumptions underlying the use of the fireball model in the optical are not as applicable in the UV. UV SN flux does not come from the Rayleigh-Jeans tail of a blackbody spectrum– the little flux emitted from the thermal photosphere is mostly absorbed by a dense forest of absorption lines from iron-peak elements (Pauldrach et al. 1996) and most of the UV light which is observed results from reverse flourescence (Mazzali 2000). We will nevertheless use the fireball model as a starting point for comparisons.

The conversion from observed count rate to flux requires a spectrum-dependent conversion factor (Poole et al. 2008) but the extreme colors of SN 2011fe at early times are beyond those previously determined (Brown et al. 2010). Since the UV SN spectrum at such early times is not well understood (Foley et al. 2011) we postpone those calculations and work with the count rates from Table 1. The left panel of Figure 2 shows the count rate curves in the first 4 days of observations along with the best fit parabolic curves. The fit parameters are given in Table 2. The UVOT b and v curves can be fit with explosion dates of August 23.8 ± 0.45 and 23.6 ± 0.26 respectively. These times are consistent with the explosion date of August 23.69 calculated by Nugent et al. (2011b) and reported via Horesh et al. (2011). Surprisingly the fireball model is a reasonable fit to the rising UV flux despite the assumptions underlying the model (Riess et al. 1999) being less supported in the UV.

Our optical data is consistent with the fireball model, extending to approximately five, five, and ten days past the explosion in the *u*, *b*, and *v* bands, respectively, before being saturated. As the UV fits are expanded to past five days after the explosion, the quality of the fits are drastically reduced, as the count rate rises quicker than the extrapolated model. For example, fitting the uvm2 count rates for the exposures less than four days after explosion, a $t_0$ of August 23.7 ± 1.05 is found, consistent with the other filters. If data between 5 and 10 days after explosion are used (more typical for early observations of SNe Ia), a larger amplitude is found and a much later $t_0$ of August 27.25 ± 0.44, which clearly does not correspond to the explosion date. Extrapolating the parabola fit to the 5-10 day observations back to the time of the earlier observations, the observed early flux would appear as an excess compared to the fireball model. Excess UV flux in the earliest observations was also found by Foley et al. (2011) in SN 2009ig when looking for shock interaction (see Section 3.3) and rejected as such.

To address the apparent change in the early slope, we introduce a second component to the fireball model:

$f = \alpha_1(t - t_{0,1})^2 + \alpha_2(t - t_{0,2})^2$

These best fit parameters are given in Table 2 for the three UV filters. The later component may be the rise of the reverse flourescence emission seen as the photosphere recedes to layers with a more favorable composition. In an attempt to simulate a possible shock breakout, we also tried a second model consisting of an early bump parameterized as a parabola with a negative amplitude superimposed on a fireball model. However, the fit gave a $\chi^2$ nearly triple that of the double fireball model and was rejected. As discussed by Foley et al. (2011) for SN 2009ig, the reddening of the colors is also inconsistent with a cooling shock.

### 3.3. *The unseen shock from a companion*

The early time UV data from SN 2011fe is also important for what is not seen – excess UV emission arising from the interaction between the SN explosion and the companion (K10). In the single degenerate Roche-lobe overflow scenario, this interaction is predicted to produce a shock that is very bright in the first few days after the explosion, particularly in the UV. In B11, we used numerical and analytic models from K10 to predict the luminosity of this shock as a function of viewing angle and companion separation distance. The analytic models give the time dependent luminosity and temperature as a function of the separation distance. From these we calculate the expected brightness of the shock in the 6 UVOT filters. The peak luminosity of the shock emission increases for larger separation distances (and thus larger stellar radii of the companion, since it assumed to fill its Roche-lobe). Thus, a 1 $M_\odot$ evolved red giant (RG) companion at a separation distance of 2 $\times 10^{13}$ cm produces more UV shock emission than main sequence (MS) stars. For all companions, the maximum shock emission occurs for a viewing angle of 0 degrees, corresponding to a geometry in which the companion lies directly in the line of sight between the observer and SN Ia.

Following the method of B11, we do not attribute any observed UV flux to the SN Ia, but instead use it as an upper limit on the early UV flux from the shock. This is necessary because the independent UV templates of M10 do not begin as early as these observations and because numerical simulations do not adequately match the observed UV light of SNe Ia (Brown et al. 2010). We determine 95% confidence lower limits on the viewing angle for each separation distance through Monte Carlo realizations that model the errors in the explosion date, photometry, distance modulus, and reddening. Further details of the analysis are found in B11.

For SN 2011fe, the very early and deep UV observations result in tighter limits on the shock luminosity than any SN Ia in B11. As with most of the SNe Ia in that sample, the strictest limits come from the first observations in the uvm2 filter. In the SN 2011fe data, the 95% upper limit on the absolute magnitude is uvm2>-9.6 mag ($\sim 5 \times 10^{-17}$ ergs s$^{-1}$ cm$^{-2}$ Å$^{-1}$) at 1.2 days after the estimated time of explosion (August 23.7 *pm* 0.1). The left panel of Figure 3 compares the observed uvm2 count rates of SN 2011fe to that predicted for a 2 $M_\odot$ companion at the distance of M101 for different viewing angles.

Lower limits on the viewing angle are determined for a range of separation distances. As shown in the right hand panel of Figure 3, the resulting lower limits on the viewing angle are 177 and 179 degrees for the 0.2 $\times 10^{13}$

(6 $M_\odot$ MS) and 2 $\times 10^{13}$ cm (1 $M_\odot$ RG) separation distance models considered in B11. By simple geometric arguments, the probability of the SNe Ia occurring at those viewing angles is negligible. For even smaller companions, we obtain lower limits of 169 and 172 degrees for companions separated by 0.05 $\times 10^{13}$ (1 $M_\odot$ MS) and 0.03 $\times 10^{13}$ cm (2 $M_\odot$ MS), with geometric probabilities of less than 1% for both. Thus MS companions with a mass greater than 2-3.5 $M_\odot$, corresponding to the super-soft x-ray sources (Li & van den Heuvel 1997; Podsiadlowski 2010), are extremely unlikely. These limits on the companion are stricter than that obtained from pre-explosion imaging by the Hubble Space Telescope (Li et al. 2011), showing the great power of these UV observations to studying the systems. The companion star could still be non-degenerate if the companion can shrink well within its Roche-lobe limit before the time of explosion (Justham 2011). Further modeling is required to determine the geometry of such systems that would still be undetected with these deep, early UV data.

## 4. SUMMARY

The early detection of SN 2011fe at such a close distance and the rapid response of *Swift* resulted in extremely early, sensitive, and densely sampled UV measurements. This allows us to extend the NUV template to a day after explosion. The early flux seems to follow a parabolic rise as suggested by the fireball model, though separate rises can be fit to the first five days and the period five to ten days after explosion. The low UV flux allows us to put very tight constraints on the existence of a single degenerate companion in Roche-lobe overflow. While most previous observations could only exclude separation distances corresponding to RG companions (Brown et al. 2011), the limits from SN 2011fe begin constraining separation distances down to a few solar radii.

These early data are a great test for the theoretical models of the early SN explosion itself. The time and magnitudes reached are comparable to that of the shock heated, expanded envelope of the WD itself (Piro, Chang, & Weinberg 2010), though a more detailed understanding of the early UV light is needed to disentangle different effects that may have been observed for the first time. Combining these data with observations across the electromagnetic spectrum (Nugent et al. 2011b; Horesh et al. 2011; Marion 2011; Smith et al. 2011) will make SN 2011fe the best studied SN Ia ever.

We are especially grateful to the Palomar Transient Factory for promptly announcing this exciting object and to Eran Ofek for initating the first *Swift* observations. This work at the University of Utah is supported by NASA grant NNX10AK43G, through the *Swift* Guest Investigator Program. This work is sponsored at PSU by NASA contract NAS5-00136. The Institute for Gravitation and the Cosmos is supported by the Eberly College of Science and the Office of the Senior Vice President for Research at the Pennsylvania State University. SRO and NPK gratefully acknowledge the support of the UK Space Agency. This analysis was made possible by access to the public data in the *Swift* data archive and the NASA/IPAC Extragalactic Database (NED). NED is operated by the Jet Propulsion Laboratory, California Institute of Technology, under contract with the National Aeronautics and Space Administration.

## REFERENCES

Breeveld, A. A., Landsman, W., Holland, S. T., Roming, P., Kuin, N. P. M., & Page, M. J. 2011, preprint, arXiv1102.4717
Brown, P. J., et al. 2005, ApJ, 635, 1192
Brown, P. J., et al. 2009, AJ, 137, 4517 (B09)
Brown, P. J., et al. 2010, ApJ, 721, 1608
Brown, P. J., et al. 2011, ApJ, submitted (B11)
Bufano, F., et al. 2009, ApJ, 700, 1456
Campana, S., et al. 2006, Nature, 442, 1008
Cenko, S. B., Thomas, R. C., Nugent, P. E., Kandrashoff, M., Filippenko, A. V., & Silverman, J. M. 2011, ATEL #3583
Cenko, S. B., Ofek, E. O., & Nugent, P. E., 2011, ATEL #3590
Foley, R. J., et al. 2011, arXiv:1109.0987
Gal-Yam, A., et al. 2011, ApJ, 736, 159
Ganeshalingam, M., Li, W., & Filippenko, A. V. 2011, MNRAS, in press
Garg, A., et al. 2007, AJ, 133,403
Gehrels, N., et al. 2004, ApJ, 611, 1005
Gezari, S., et al. 2008, ApJ, 683, 131
Hayden, B. T., et al. 2010, ApJ, 712, 350
Hom, A. V., Wu, C, & Caldwell, J. J. 1974, PASP, 86, 296
Horesh, A., et al. 2011, ApJ, submitted, arXiv:1109:2912
Immler, S. 2006, ApJL, 648, 119
Justham, 2011, ApJL accepted, arXiv:1102.4913
Kasen, D. 2010, ApJ, 708, 1025
Kirshner, R. P., et al. 1993, ApJ, 415, 589
Law, N. M., et al. 2009, PASP, 121, 1395
Li, W., et al. 2011, Nature, submitted, arXiv:1109.1593
Li, X. D. & van den Heuvel, E. P. J. 1997, A&AL, 322, 9
Margutti, R. & Soderberg A. 2011, ATEL #3584
Marion, H. 2011, ATEL #3599
Mazzali, P. A. 2000, A&A, 363, 705
Milne, P., et al. 2010, AJ, 721, 1627
Nugent, P., Sullivan, M., Bersier, D., Howell, D. A., Thomas, R., & James, P. 2011, ATEL #3581
Nugent, P., et al. 2011, Nature, submitted
Panagia, N. 2003, in Supernovae and Gamma-Ray Bursters, ed. K. Weiler (Berlin: Springer), 113
Pauldrach, A. W. A., Duschinger, M., Mazzali, P. A., Puls, J., Lennon, M., & Miller, D. L. 1996, A&A, 312, 525
Piro, A. L., Chang, P. & Weinberg, N. N. 2010, ApJ, 708, 598
Podsiadlowski, P. 2010, AN, 331, 218
Poole, T. S., et al. 2008, MNRAS, 383, 627
Riess, A. G., et al. 1999, AJ, 118, 2675
Roming, P. W. A., et al. 2005, Space Science Reviews, 120, 95
Roming, P. W. A., et al. 2009, ApJL, 704, 118
Schlegel, D. J., Finkbeiner, D. P., & Davis, M. 1998, ApJ, 500, 525
Shappee, B. J., & Stanek, K. Z. 2011, ApJ, 733, 124
Smith, P., Smith, N., Milne, P., & Williams, G. 2011, ATEL 3612
Soderberg, A. M., et al. 2008, Nature, 453, 469
Thomas, R. C., et al. 2011, ApJ, in press, arXiv1109.1312

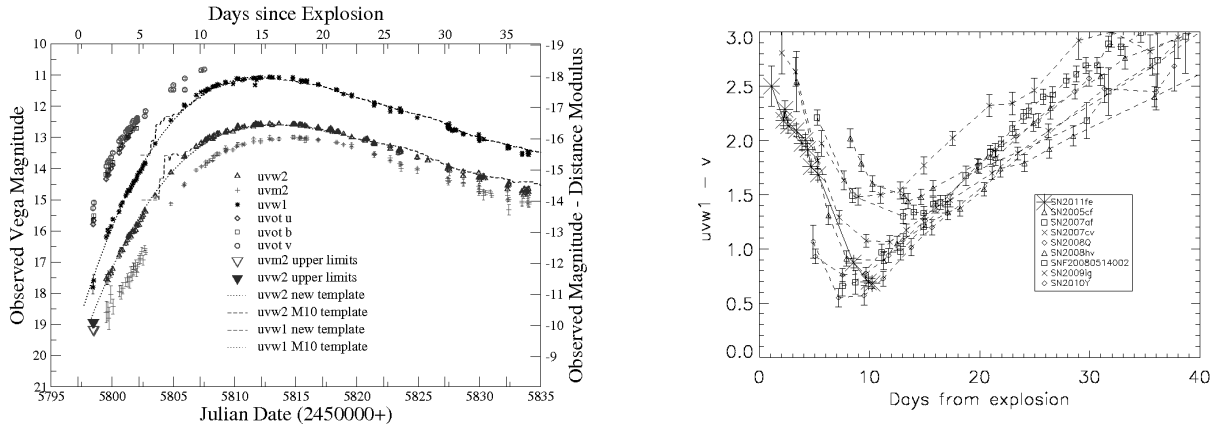


FIG. 1.— *Left:* UVOT light curves of SN 2011fe in Vega magnitudes. The M10 templates for uvw1 and uvw2 are overplotted with dashed lines and the new pre-maximum templates derived from these observations are marked with dotted lines. *Right:* uvw1-v color curves for a sample of normal SNe observed within 10 days of explosion.

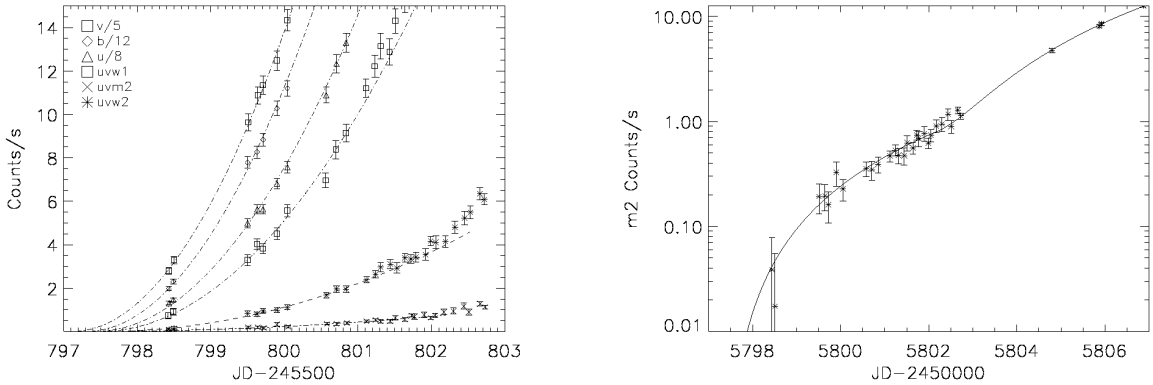


FIG. 2.— Left: Early count rates in the 6 UVOT filters along with the best fit parabolic curves. Right: Early count rates in the uvm2 filter fit with a two component fireball model.

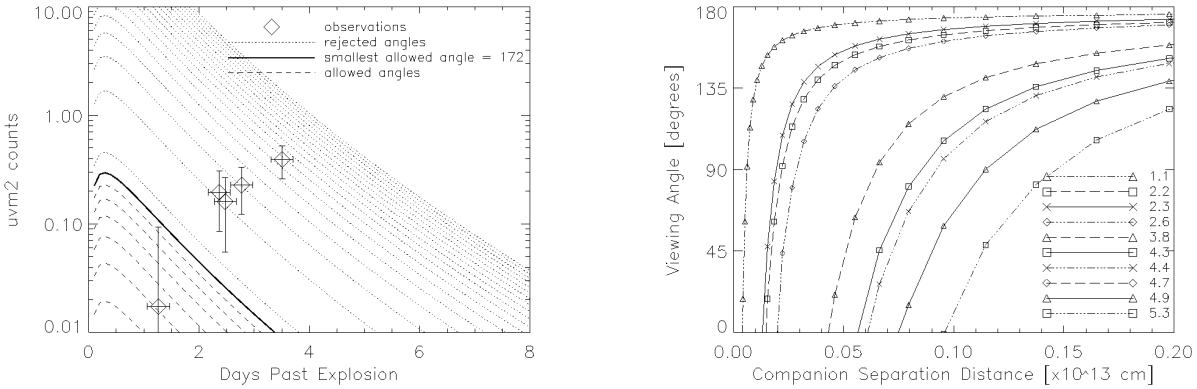


FIG. 3.— *Left:* Observed uvm2 count rates (with 95% errors on the luminosity (from measured count rate, distance, and extinction) and 0.2 day uncertainty on the explosion date) from the first 5 exposures compared to the predicted count rates (K10,B11) for the 2 $M_\odot$ MS companion at a separation distance of 5 $\times 10^{11}$ cm for various viewing angles. Viewing angles at greater than 172 degrees are allowed (shown as dashed lines separated by one degree intervals), while those with smaller angles (from 0 to 170 degrees separated 10 degrees) are rejected at 95% confidence. The rejected angles conflict with the first observation, and one can see that for this separation distance smaller viewing angles (and similarly for a fixed viewing angle larger separations) would have been allowed if the observations had not begun so soon.
*Right:* Separation distance-viewing angle constraints for SN 2011fe from the uvm2 filter for different epochs (given in the legend in days past explosion). The regions under the curve are excluded at 95% confidence by that particular observation.

TABLE 1
SN2011FE PHOTOMETRY

| Filter | JD-2450000 | Mag | Count Rate |
|---|---|---|---|
| uvm2 | 5798.44 | >19.15 | 0.04 ± 0.04 |
| uvm2 | 5798.51 | >19.17 | 0.02 ± 0.04 |
| uvm2 | 5799.51 | 18.61 ± 0.35 | 0.19 ± 0.06 |
| uvm2 | 5799.64 | 18.59 ± 0.31 | 0.2 ± 0.05 |
| uvm2 | 5799.72 | 18.81 ± 0.36 | 0.16 ± 0.05 |
| uvm2 | 5799.9 | 18.04 ± 0.28 | 0.33 ± 0.08 |

NOTE. — The full table of photometry is available in the electronic version.

TABLE 2
EARLY COUNT RATE FITS

| Filter | Range | $\alpha_1$ | $t_0$ | $\alpha_2$ | $t_{0,2}$ | $\chi^2$/(N-P)[a] |
|---|---|---|---|---|---|---|
| uvw2 | 1-4 days | 0.18 ± 0.04 | 5797.52 ± 0.50 | ··· | ··· | 2.83/ ( 11-2) |
| uvm2 | 1-4 days | 0.03 ± 0.02 | 5797.33 ± 1.05 | ··· | ··· | 3.34/ ( 11-2) |
| uvw1 | 1-4 days | 0.78 ± 0.19 | 5797.44 ± 0.53 | ··· | ··· | 10.44/ ( 11-2) |
| *u* | 1-4 days | 8.68 ± 1.77 | 5797.34 ± 0.42 | ··· | ··· | 10.94/ ( 11-2) |
| *b* | 1-4 days | 18.50 ± 4.04 | 5797.29 ± 0.45 | ··· | ··· | 8.55/ ( 10-2) |
| *v* | 1-4 days | 6.69 ± 0.83 | 5797.12 ± 0.26 | ··· | ··· | 2.90/ ( 11-2) |
| uvw2 | 5-10 days | 0.88 ± 0.09 | 5800.03 ± 0.23 | ··· | ··· | 7.97/ ( 10-2) |
| uvm2 | 5-10 days | 0.31 ± 0.06 | 5800.77 ± 0.44 | ··· | ··· | 19.99/ ( 9-2) |
| uvw1 | 5-10 days | 4.50 ± 0.82 | 5800.09 ± 0.39 | ··· | ··· | 22.32/ ( 10-2) |
| uvw2 | 1-10 days | 0.20 ± 0.02 | 5797.64 ± 0.23 | 0.96 ± 0.15 | 5801.70 ± 0.45 | 13.04/ ( 32-4) |
| uvm2 | 1-10 days | 0.03 ± 0.01 | 5797.38 ± 0.59 | 0.43 ± 0.09 | 5802.19 ± 0.57 | 21.83/ ( 31-4) |
| uvw1 | 1-10 days | 0.97 ± 0.10 | 5797.70 ± 0.25 | 5.11 ± 0.91 | 5801.59 ± 0.51 | 38.14/ ( 32-4) |

[a] The degrees of freedom are given as the number of points (N) minus the number of fit parameters (P)